MIMO Antenna with Pattern Reconfiguration and Correlation Reduction for WLAN Applications

Sagiru Gaya, Oludayo Sokunbi, Abubakar Hamza, Sharif I. Sheikh, and Hussein Attia
Electrical Engineering department, King Fahd University of Petroleum and Minerals (KFUPM), Dhahran 3126, Saudi Arabia. Corresponding author: Hussein Attia

Abstract—In this paper, a novel beam steerable 2.4 GHz MIMO antenna array is proposed based on the Yagi-Uda principle. The antenna consists of two co-axially excited patch radiators with modified ground plane. A conducting strip with an integrated PIN diode is optimally placed between the patch radiators to act as a director or a reflector to steer the main beam by an angle of +/- 60°. For all switching modes, the MIMO antenna demonstrates an average gain and efficiency of 5 dB and 92%, respectively, at the resonance frequency of 2.4 GHz. Reduced envelope correlation coefficient in one switching mode exhibited 17 dB improvement in mutual isolation. The simulated results agreed well with measured data. This simple, low-cost, efficient, and mutually isolated antenna array can be very useful in MIMO WLAN applications.

1. INTRODUCTION

Multiple-input multiple-output (MIMO) technology has been recently used by antenna engineers to increase signal to noise ratio, spectrum efficiency and channel capacity especially in a multipath environment [1] - [3]. Also, because of the emerging handheld nature of smart devices, patch antennas have been commonly used in MIMO antennas because of their simplicity and flexibility. However, MIMO patch antennas usually suffer from mutual coupling because of the undesired surface waves radiating inside the substrate, space waves transmitted among individual elements of the array, as well as the surface waves propagating through the ground plane [4]. This coupling increases as the antenna elements are brought close to each other, with the aim of maximising space for other electronic components. This can adversely affect the throughput as well as the efficiency of the antenna array [4]. Also, increasing wireless system capacity without increasing the available bandwidth is always limited by the correlation of the antenna elements [4].

Mutual coupling has been proved to be mitigated in MIMO antennas by the use of decoupling structures [5] - [6]. Some of the decoupling methods used in literature include metamaterial structures and defective ground plane applied to increase the isolation between two patch antennas by 10-40 dB in the frequency range of 4.0-6.5 GHz [5]. Also, in [6], 8-11 dB isolation improvement was accomplished using double-layer metamaterial absorber between four patch antennas at 1.26 GHz. Fractal decoupling structure was used by [7] to accomplish 8-32 dB mutual coupling reduction between 3.17-4.15 GHz. The authors in [8] placed a resistor between four parallel-coupled resonators to achieve 25 dB isolation between 6-7 GHz. In [9], meander lines and H-shaped strips were used to achieve about 27 dB isolation improvement in the 11.8% operational bandwidth of a patch antenna array. Near field resonators are used to achieve about 20 dB isolation in two patch antennas around 2.23 GHz [10]. Three-element E-plane array antennas are decoupled with the use of metal vias and defected ground surface to obtain maximum of 16.6 dB in the 3.95-4.04 GHz impedance bandwidth [11]. A 27 dB isolation improvement was observed when inter-digital lines are placed between two patch antennas at 5.8 GHz [12]. Also, in [13], a novel hybrid electromagnetic structure and defected ground surface were used to achieve 22 dB isolation between two patch antennas at 4.9 GHz. In [14], Sokunbi et al. used slotted-EBG structure to isolate MIMO patch antenna array at millimeter-wave frequency.

Radiation patterns correlation reduction is also employed to improve the antenna efficiency by minimizing the envelope correlation coefficient (ECC) of the elements [15]. In literature, PIN diode

switches are widely used to implement MIMO antennas with reduced ECC and mutual coupling. For example, in [16], fixed dipole lengths are manipulated to reconfigure radiation patterns with improved mutual isolation and minor changes in the antenna efficiency. Also, in [17], high isolation, low ECC and three switchable beams using four PIN diodes are reported for a reconfigurable MIMO antenna. In [18], 8 PIN diodes are integrated into a MIMO microstrip U-slot antenna to achieve dual switched beams with a mutual coupling of -20 dB in all switched modes. In [19], the authors utilized six PIN diodes to achieve seven scanning angles, using a simple printed antenna array with efficiency of more than 85% maintained throughout all the switching modes. It is noteworthy that most of the aforementioned designs either employs sophisticated structures [4] - [6], [14] or demonstrate low efficiency [17] - [18].

In this paper, a microstrip MIMO antenna designed using the Yagi-Uda principle is proposed. The antenna comprises two driven elements and one parasitic element that are coupled through near-field and surface waves. The dimensions of the driven elements are dependent on the antenna resonant frequency. Whereas the dimensions of the parasitic element are controlled electronically using PIN-diodes to act as a director or reflector depending on their lengths, based on the Yagi-Uda approach. Hence, the phase delay between the driven and parasitic elements introduce the desired tilt in the main beams. Two square patches with modified ground planes are used here as driven elements of the 2.4 GHz MIMO antenna. A conductor strip with an integrated PIN diode is used as a switched parasitic element and optimally placed between the driven elements. Consequently, the main beams of the driven elements are steered in the desired direction based on the switching state of the diode. Numerical results obtained using the CST commercial simulation tool are verified with measured S-parameters and radiation patterns.

2. RECONFIGURABLE MIMO ANTENNA DESIGN

This section explains the design and operational principles of the proposed antenna. The proposed MIMO pattern reconfigurable antenna depicted in Fig. 1 is designed using the Yagi-Uda principle [20] - [21] for microstrip structures, where constructive mutual coupling between the driven and parasitic elements is maintained, and destructive mutual coupling between the two driven elements is suppressed. The parasitic element located midway between the two driven elements (see Fig. 1(a)) acts as a reflector when its integrated PIN diode is switched ON, hence, the reflector tilts the radiated beam. The parasitic element also acts as a director when the diode is switched OFF. The Yagi-Uda approach specifically requires that the reflector or director be located at a quarter wavelength distance from the middle of the driven element [20].

Figure 1 shows the simple 2.4 GHz antenna structure, consisting of two square driving element with the dimensions of w_p and separated by $L_r = 26.7$ mm or $0.22\lambda_0$ (λ_0 is the free space wavelength at 2.4 GHz). A rectangular copper strip of dimensions L_d x d with an integrated PIN diode is placed equidistantly from the two driving elements and at $S = 30$ mm from the middle of each patch. When the switch is ON, the strip is serving two functions: firstly, it acts as a reflector of the Yagi-Uda structure, because its length is longer than the driven patches; secondly, it acts as a decoupling structure for the two MIMO patch elements. The antenna is printed on Rogers RO3003 substrate with dielectric constant of 3, loss tangent of 0.001 and thickness 1.52 mm. Figure 1(b) shows the partial ground plane of the two-element MIMO antenna with dimensions $L_g \times W_g$. The pattern reconfiguration ability of the antenna depends on the width (W_g) of the partial ground that needs to be less than the length of the reflector as explained in the next section. It is noteworthy that the width of the reflector (d) should be approximately $0.05\lambda_0$ for maximum deflection of the radiated beams. Employing the commercial numerical CST tool, the thoroughly optimized dimensions of the radiating system are $L_s = 105$ mm, $W = 55$ mm, $L_r = 26.7$ mm, $L_d = 49.2$ mm, $W_p = 34.8$ mm, $d = W_g = 6$ mm, $L_g = 43.8$ mm, $L_p = 26.5$ mm.

3. RESULTS AND DISCUSSION

This session elucidates on the simulated and measured results of the proposed antenna structure. According to the Yagi-Uda principle, the proposed antenna in Fig. 1 is simulated and analyzed for both states of the diode switch. When the switch is OFF, the parasitic element acts as a director as its length is shorter than that of the driven elements. But during the ON state, the strip acts as a reflector

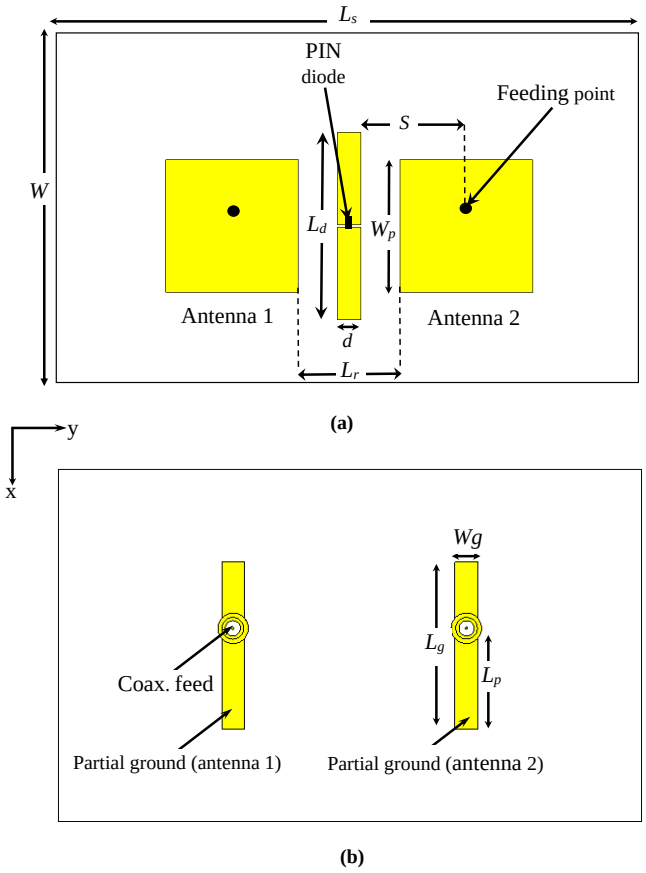

Figure 1: Proposed pattern reconfigurable MIMO antenna: (a) Top view, and (b) Back view.

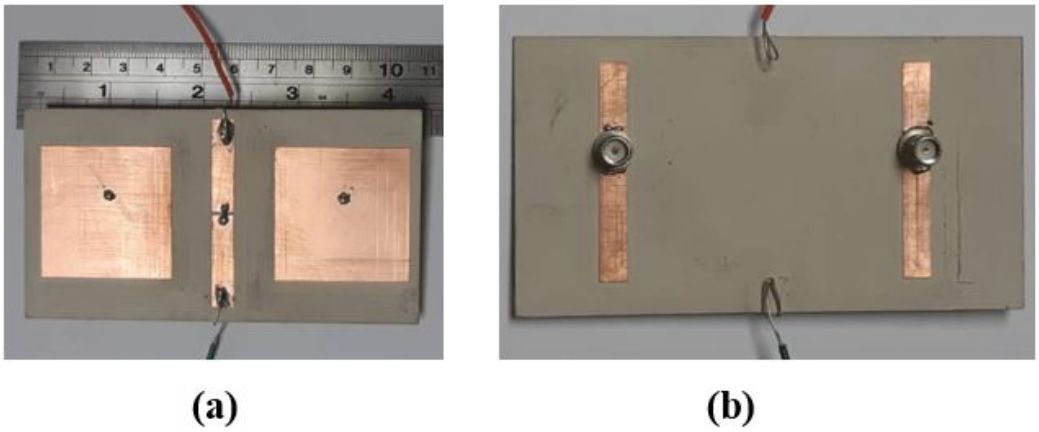

Figure 2: Fabricated pattern reconfigurable MIMO antenna: (a) Top view, and (b) Back view.

because its length becomes longer than that of the two driven elements. Figure 2 depicts the top and back view of the fabricated prototype.

The simulated and measured reflection coefficient of the ON and OFF states are depicted in Fig. 3. It is obvious that the antenna resonates around 2.4 GHz with a good agreement between the measured and simulated results for both ON and OFF states. Figure 4 depicts the simulated and measured isolation of the MIMO antenna in both the OFF and ON states of the PIN diode. When the diode is switched ON by applying a DC bias voltage of 0.707 v, about 17 dB isolation improvement is noticed

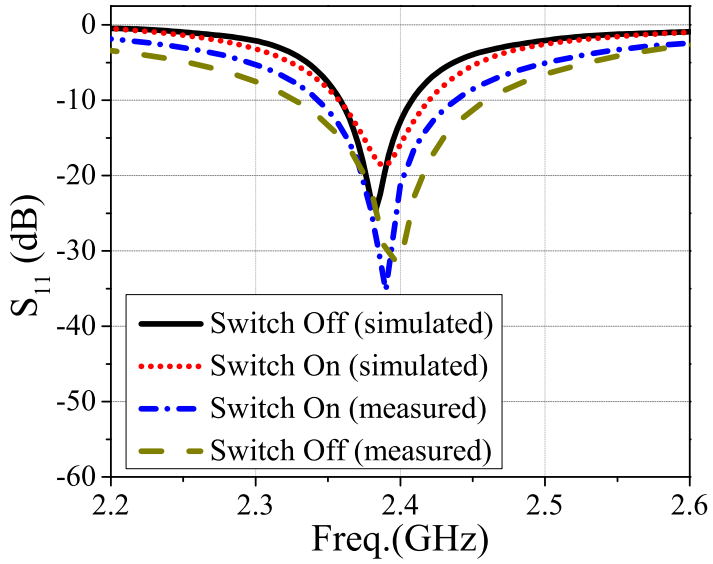

Figure 3: Simulated and measured reflection coefficients of the proposed pattern reconfigurable MIMO antenna.

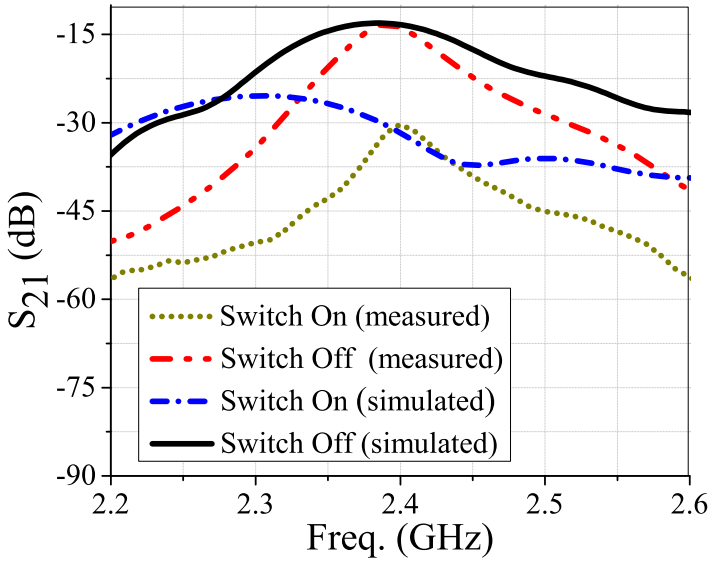

Figure 4: Simulated and measured transmission coefficients of the proposed pattern reconfigurable MIMO antenna.

between the two MIMO antenna elements at the design frequency of 2.4 GHz. This improvement can be attributed to the fact that the printed line between the two MIMO antennas is serving as a suppressor of the surface wave and deflector of the radiated waves.

Also, the measured S_{21} reasonably agrees with the simulated results, especially at the resonant frequency of 2.4 GHz. The discrepancy between the simulation and measurement results are attributed

Table 1: Switching modes for the MIMO reconfigurable antenna

Switch state	Antenna 1 beam angle	Antenna 2 beam angle
OFF	-30°	30°
ON	-60°	60°

to the different characteristics of the substrate material used in simulation and fabrications, and due to the existence of the PIN diode that was modeled as RLC circuit in the CST numerical simulations.

It should be noted that the DC biasing lines usually used with PIN diodes are not needed here since the AC excitation from the coaxial feed is already separated from the PIN diode. Table 1 summarizes the switching states of the MIMO antenna.

3.1. Radiation Patterns of the MIMO Antenna

The beam deflection can be proven by the H-plane (i.e., Y-Z plane) radiation patterns of the two MIMO antennas as demonstrated in Fig. 5 at 2.4 GHz. Note that When the diode is OFF, the main beams of the two antennas are directed at - 30° (antenna 1) and 30° (antenna 2). But when the diode is ON, the reflector element (i.e., strip line) further deflects the radiation patterns of the two antennas, hence, the angles of antenna 1 tilts to - 60° while antenna 2 tilts to 60°. This extra 30° tilt in both antennas is responsible for the 17 dB reduction in mutual coupling as shown in Fig. 4. Therefore, by using just one PIN diode, the MIMO antenna is able to achieve independent beams at four scanning angles, as well as isolation improvement. It is clear from Fig. 5 that the measured results match the simulated results.

3.2. Effect of the Ground Plane

The tilting angles of the radiated beam is highly depended on the ground plane's dimensions. Any change in the width W_g of the the ground plane disrupts the beam angle. If the substrate is fully backed with a ground plane, the radiated beam would tilt towards 0° irrespective of the switching mode because the ground plane will be the main reflector in this case. Fig. 6 depicts the effect of altering the width of the partial ground plane for the OFF state of antenna 2 which is supposed to be deflected at 30° as shown in Table 1. It is obvious that as the width of the ground plane decreases, the beam tilting increases towards the intended direction of 30°. This effect is also noticeable for other switching modes. It is also observed that the beam angle slightly changes when the width W_g of the ground plane is less than 10 mm. Hence, 6 mm has been chosen as the width of the partial ground of the proposed antenna as this results in a narrower beam width. Moreover, it has also been observed that the length L_g of the ground plane also affects the switching ability of the antenna, just like the behaviour of the width W_g, the smaller the length of the partial ground, the higher the beam angle. The length of the ground plane L_g has been assigned to be 43.8 mm which is smaller than the length of the parasitic line L_g= 49.2 mm in order to properly scan the beam in the required direction. Although the width of the ground plane significantly affects the radiation patterns of the antenna, it however, slightly affects the resonance frequency as depicted in Fig. 7. For any size of the ground plane, the antenna resonates around 2.4 GHz. The poor matching at some of the ground widths is due to the change in the matching position of the coaxial feedline as the ground size increases or decreases.

3.3. Surface Current Distribution

The surface current distribution over the MIMO antenna array for both switching modes is depicted in Fig. 8 when only antenna 1 is excited. From Fig. 8(a), most of the surface currents emanating from antenna 1 is coupled to antenna 2 when the diode is OFF. However, when the diode is ON, the reflector further tilts the beam of antenna 1 and thus preventing most of the surface current from getting to antenna 2, thereby, increasing the isolation as shown in Fig. 8(b). The beam tilting is obvious because of the low surface current shown in antenna 2 as antenna 1 is excited. If antenna 2 is excited, the same scenario will occur, with more surface current evident in antenna 2 and less surface current in antenna 1.

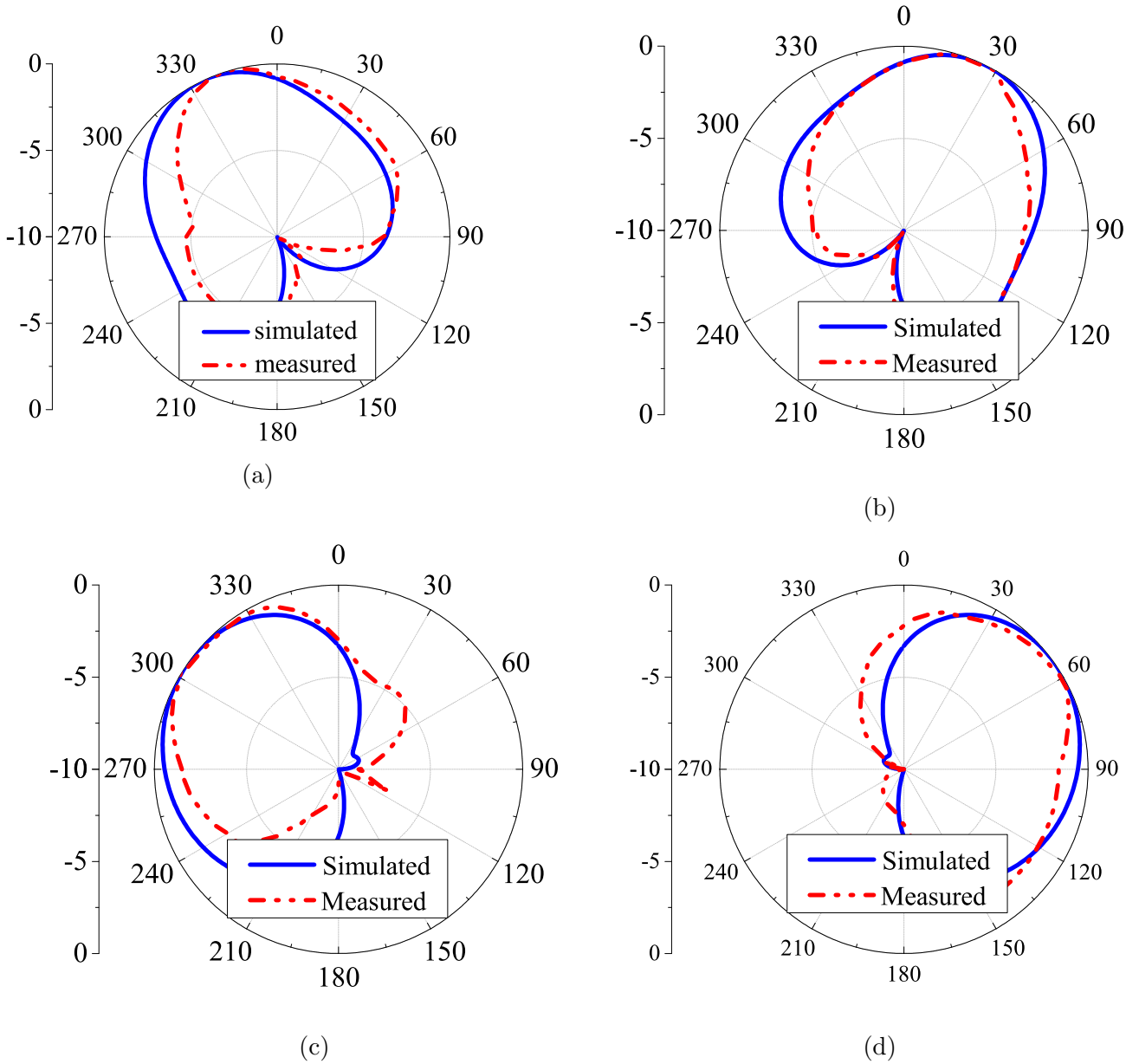

Figure 5: Radiation patterns of the proposed pattern reconfigurable MIMO antenna at 2.4 GHz: (a) Antenna 1 when switch is OFF, (b) Antenna 2 when switch is OFF (c) Antenna 1 when switch is ON, and (d) Antenna 2 when switch is ON.

3.4. Envelope Correlation Coefficient(ECC)

To further verify the isolation-improvement capability of the proposed MIMO antenna, the ECC, which is an important performance criteria in MIMO antenna is studied. The ECC can be calculated based on the S-parameters or the far-field characteristics of the antenna. ECC based on far-field considers the radiated beam direction while ECC based on S-parameters considers the ports characteristics of the two antennas. ECC based on far-field properties is considered more indicative of the isolation quality although costly because of the need to measure the radiation patterns of the antenna. ECC values less than 0.4 is generally considered acceptable for MIMO antennas. The ECC based on S-parameters is calculated using [22]:

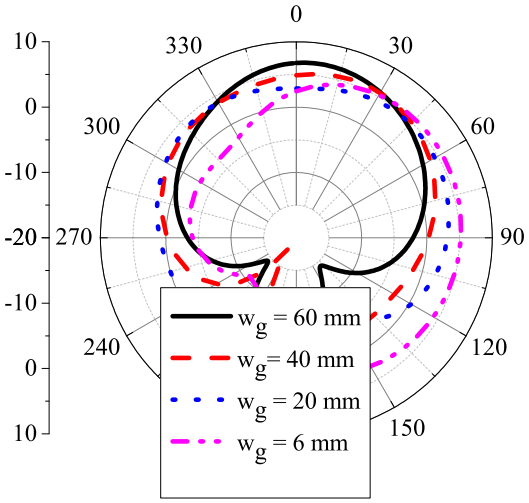

Figure 6: Effect of the ground plane width on the radiation pattern.

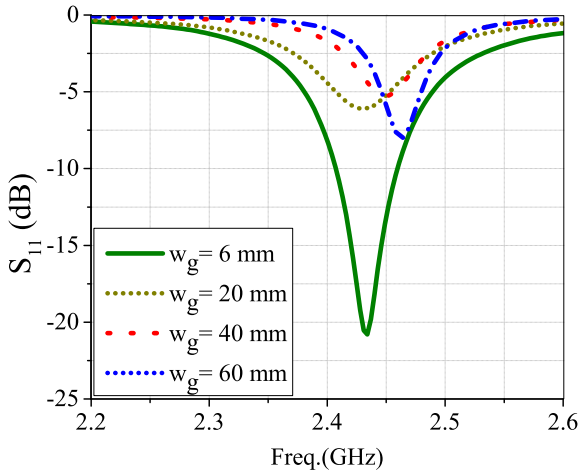

Figure 7: Effect of the ground plane width on the reflection coefficient.

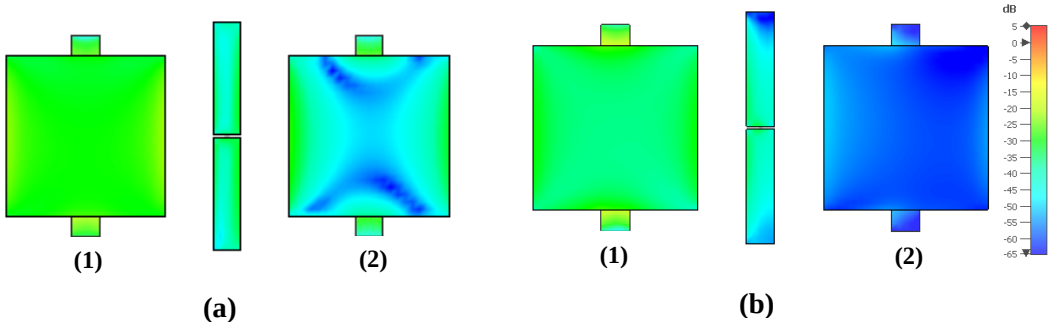

Figure 8: Surface current distribution of the proposed MIMO reconfigurable antenna array when (a) switch is OFF, and when (b) switch is ON.

$$ECC = \frac{|S_{11}{}^{*}\ S_{12} + S_{21}{}^{*}\ S_{22}|^2}{|(1 - |S_{11}{}^2| - |S_{21}{}^2|)(1 - |S_{12}{}^2| - |S_{22}{}^2|)|} \quad (1)$$

The ECC based on far-field is calculated using [22]:

$$ECC = \frac{|\iint_{4\pi}[A_1(\theta,\phi) * A_2(\theta,\phi)]d\Omega|^2}{\iint_{4\pi}|A_1(\theta,\phi)|^2 d\Omega \iint_{4\pi}|A_2(\theta,\phi)|^2 d\Omega} \quad (2)$$

where $A_1(\theta,\phi)$ is the field pattern when antenna 1 is fed and antenna 2 is terminated by 50 Ω load.

From Fig. 9, it is clear that the ECC based on far-field is around -22 dB at the resonant frequency of 2.4 GHz when the switch is OFF and around -27 dB when the switch is ON, thus, having an improvement of about 5 dB. Also, the ECC based on S-parameters is demonstrated in Fig. 10. It can be observed from Fig. 10 that the ECC based on S-parameter is about -22 dB when the diode is switched OFF and about -41 dB when the diode is switched ON at the resonant frequency of 2.4 GHz, thus, having an improvement of 19 dB. These results highly indicate that the mutual coupling between the two antennas can be effectively mitigated by switching the diode ON.

3.5. MIMO Antenna Efficiency and Gain

The simulated radiation efficiency and gain of the proposed MIMO antenna is depicted in Fig. 11 and Fig. 12, respectively. It is evident from Fig. 11 that the antenna exhibits radiation efficiency of about 93% when the diode is switched OFF and about 91% when the diode is switched ON at the resonant frequency of 2.4 GHz. This slight decrease in efficiency is as a result of the employment of electronic components (i.e., PIN diode) which usually degrades the efficiency of antennas. However, from Fig. 12, the antenna exhibits a gain of about 4.5 dBi when the diode is switched OFF and 5.4 dBi when the diode is switched ON, thus, having a slight improvement. The increase in the antenna gain is a result of the mutual coupling reduction between the two driven radiating elements. The reduced mutual coupling is as a result of the deflection of the antennas' beams in opposite directions when the employed electronic switch is switched ON.

4. CONCLUSION

This paper presents a simple and efficient pattern reconfigurable microstrip MIMO antenna array that consists of two square driven elements placed on both sides of a rectangular parasitic element. By optimizing the ground plane size and the location of the shared parasitic element, the designed antenna demonstrated four scanning beams with just a single diode switch. The effect of the width of the ground plane on the radiation characteristics of the antenna, as well as the resonance frequency of the antenna have been analyzed. By turning the switch on, 30° beam tilting increase is observed in the radiation patterns of both driven elements, as well as 17 dB isolation improvement between the two driven elements. For both switching modes of the proposed MIMO antenna, the ECC values based on far-fields and S-parameters are better than -20 dB. Also, there was a slight increase in the antenna gain. Measured results agreed well with the simulated data. This simple but yet efficient antenna is an excellent candidate for MIMO WLAN applications.

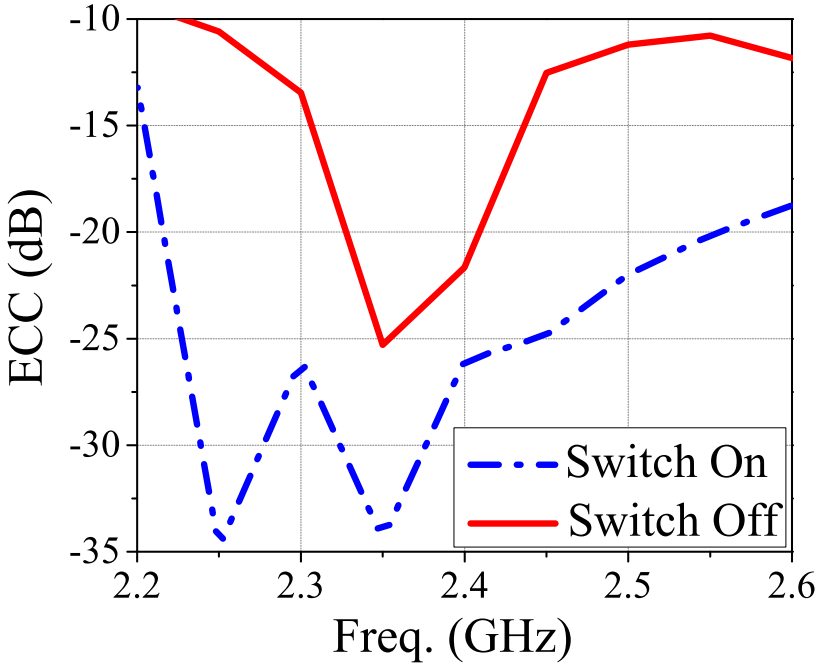

Figure 9: Envelope correlation coefficient (ECC) of the proposed pattern reconfigurable MIMO antenna based on far-field results.

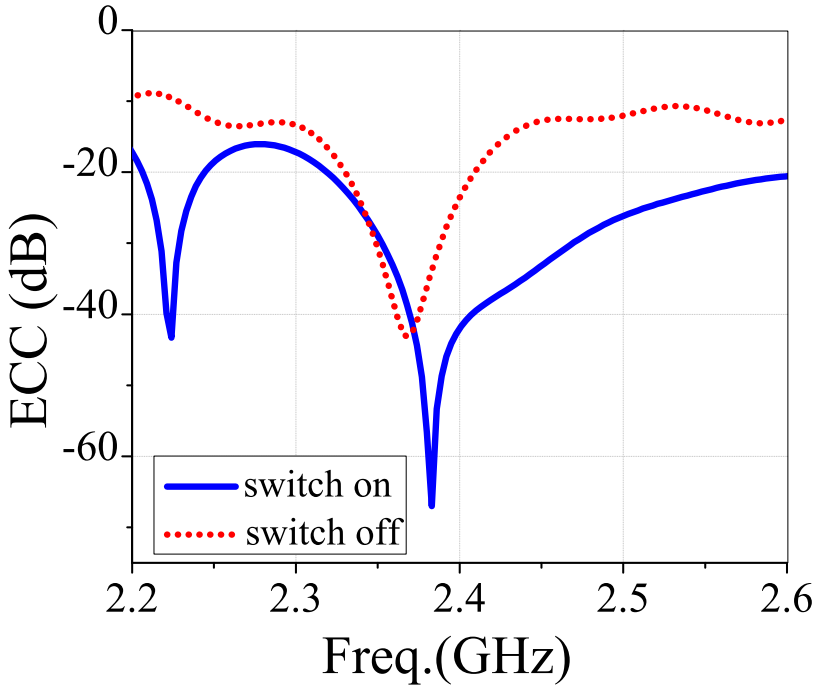

Figure 10: Envelope correlation coefficient (ECC) of the proposed pattern reconfigurable MIMO antenna based on S-parameters.

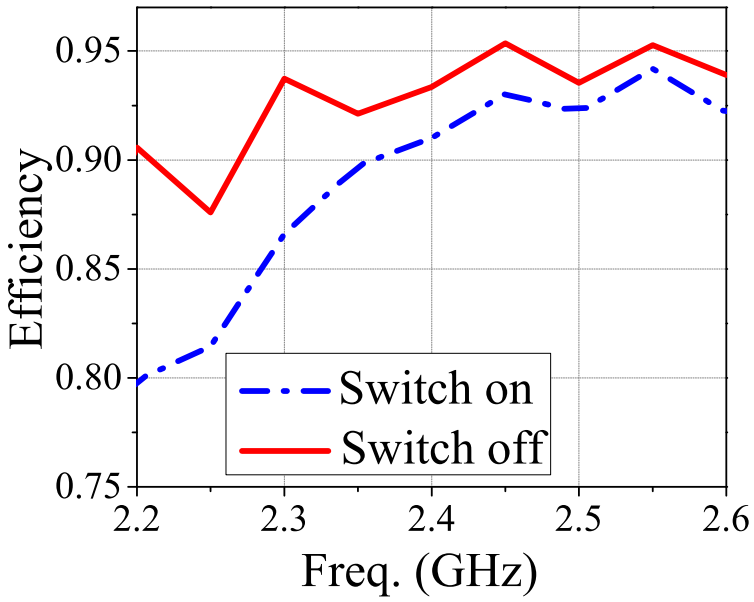

Figure 11: Radiation efficiency of the proposed MIMO pattern reconfigurable antenna.

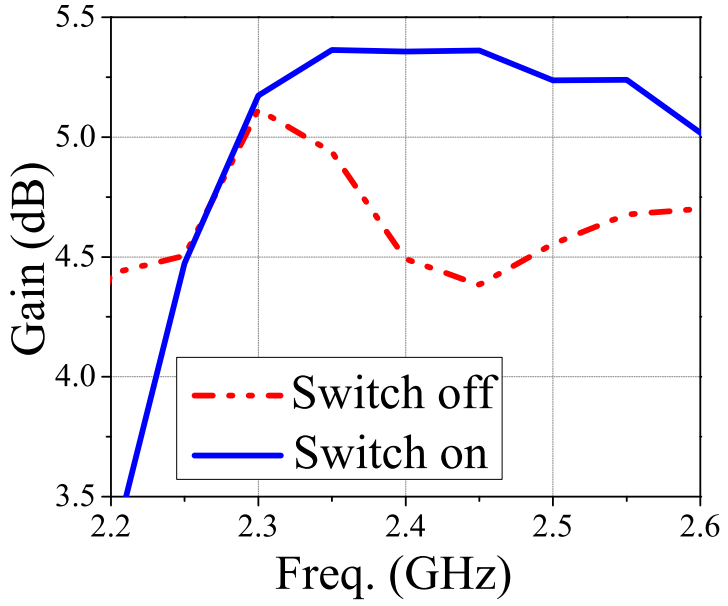

Figure 12: Gain of the proposed MIMO pattern reconfigurable antenna.

Acknowledgment

The authors are grateful for the financial support provided by King Fahd University of Petroleum and Minerals (KFUPM) under project No. GTEC1802.

conflict of interest

Authors have no conflict of interest relevant to this article.

REFERENCES

1. Y. Zhang, S. Zhang, J. Li, and G. F. Pedersen, "A transmission-line-based decoupling method for mimo antenna arrays," *IEEE Transactions on Antennas and Propagation*, vol. 67, no. 5, pp. 3117–3131, May 2019.
2. C. You, D. Jung, M. Song, and K. Wong, "Advanced coupled-fed mimo antennas for next generation 5g smartphones," in *2018 International Symposium on Antennas and Propagation (ISAP)*, Oct 2018, pp. 1–2.
3. M. Li, B. G. Zhong, and S. W. Cheung, "Isolation enhancement for mimo patch antennas using near-field resonators as coupling-mode transducers," *IEEE Transactions on Antennas and Propagation*, vol. 67, no. 2, pp. 755–764, Feb 2019.
4. X. Chen, S. Zhang, and Q. Li, "A review of mutual coupling in mimo systems," *IEEE Access*, vol. 6, pp. 24 706–24 719, 2018.
5. O. Sokunbi and H. Attia, "Highly reduced mutual coupling between wideband patch antenna array using multiresonance ebg structure and defective ground surface," *Microwave and Optical Technology Letter*, pp. 1–10, 2019.
6. J. Zhang, J. Li, and J. Chen, "Mutual coupling reduction of a circularly polarized four-element antenna array using metamaterial absorber for unmanned vehicles," *IEEE Access*, vol. 7, pp. 57 469–57 475, 2019.
7. X. Li, G. Yang, and Y. Jin, "Isolation enhancement of wideband vehicular antenna array using fractal decoupling structure," *IEEE Antennas and Wireless Propagation Letters*, vol. 18, no. 9, pp. 1799–1803, Sep. 2019.
8. J. Park, M. Rahman, and H. N. Chen, "Isolation enhancement of wide-band mimo array antennas utilizing resistive loading," *IEEE Access*, vol. 7, pp. 81 020–81 026, 2019.
9. Z. Chen, M. Li, G. Liu, Z. Wu, and M. Tang, "Isolation enhancement for wideband, circularly/dual-polarized, high-density patch arrays using planar parasitic resonators," *IEEE Access*, vol. 7, pp. 112 249–112 257, 2019.
10. M. Li, B. G. Zhong, and S. W. Cheung, "Isolation enhancement for mimo patch antennas using near-field resonators as coupling-mode transducers," *IEEE Transactions on Antennas and Propagation*, vol. 67, no. 2, pp. 755–764, Feb 2019.
11. Z. Niu, H. Zhang, Q. Chen, and T. Zhong, "Isolation enhancement for 1×3 closely spaced e-plane patch antenna array using defect ground structure and metal-vias," *IEEE Access*, vol. 7, pp. 119 375–119 383, 2019.
12. H. Qi, X. Yin, L. Liu, Y. Rong, and H. Qian, "Improving isolation between closely spaced patch antennas using interdigital lines," *IEEE Antennas and Wireless Propagation Letters*, vol. 15, pp. 286–289, 2016.
13. Y. Liu, X. Yang, Y. Jia, and Y. J. Guo, "A low correlation and mutual coupling mimo antenna," *IEEE Access*, vol. 7, pp. 127 384–127 392, 2019.
14. O. Sokunbi, H. Attia, and S. I. Sheikh, "Microstrip antenna array with reduced mutual coupling using slotted-ring ebg structure for 5g applications," in *2019 IEEE International Symposium on Antennas and Propagation and USNC-URSI Radio Science Meeting*, July 2019, pp. 1185–1186.
15. A. Elshirkasi, A. Al-Hadi, M. Mansor, R. Khan, and P. Soh, "Envelope correlation coefficient of a two-port mimo terminal antenna under uniform and gaussian angular power spectrum with user's hand effect," *Progress In Electromagnetics Research C*, pp. 123–136, 2019.
16. G. D. Sworo, D. Patron, K. R. Dandekar, and M. Kam, "Characterization of pattern reconfigurable antenna arrays for mimo systems," in *2015 49th Annual Conference on Information Sciences and Systems (CISS)*, March 2015, pp. 1–3.
17. C. Rhee, Y. Kim, T. Park, S. Kwoun, B. Mun, B. Lee, and C. Jung, "Pattern-reconfigurable mimo

antenna for high isolation and low correlation," *IEEE Antennas and Wireless Propagation Letters*, vol. 13, pp. 1373–1376, 2014.

18. P. Qin, Y. J. Guo, A. R. Weily, and C. Liang, "A pattern reconfigurable u-slot antenna and its applications in mimo systems," *IEEE Transactions on Antennas and Propagation*, vol. 60, no. 2, pp. 516–528, Feb 2012.
19. S. Gaya, R. Hussain, M. Sharawi, and H. Attia, "Pattern reconfigurable yagi-uda antenna with seven switchable beams for wimax application," *Microwave and Optical Technology Letter*, pp. 1–6, 2019.
20. Y. Mushiake, "A theoretical analysis of the multi-element end-fire array with particular reference to the yagi-uda antenna," *IRE Transactions on Antennas and Propagation*, vol. 4, no. 3, pp. 441–444, July 1956.
21. C. A. Balanis, *Antenna theory: analysis and design.* Wiley-Interscience, 2005.
22. S. Blanch, J. Romeu, and I. Corbella, "Exact representation of antenna system diversity performance from input parameter description," *Electronics Letters*, vol. 39, no. 9, pp. 705–707, May 2003.